Journal of Engineering Science and Technology
Vol. 13, No. 1 (2018) 226 - 241

EXPERIMENTAL STUDY ON CURVED COMPOSITE I-GIRDER BRIDGE SUBJECTED TO IRAQI LIVE LOADING FOR ROAD BRIDGES

AMER F. IZZET*, AYMEN R. MOHAMMED

Civil Engineering Department, College of Engineering, Baghdad University, Baghdad, Iraq
Middle Technical University, Baghdad, Iraq
*Corresponding Author: amer.f@coeng.uobaghdad.edu.iq

Abstract

Experimental programme was carried out to investigate the flexural behaviour of horizontally curved composite I-girder decks subjected to Iraqi Standard bridge live loads. This program included fabricating and testing five scaled-down, simply supported, curved bridge models, 3 m in central span length. Each model included four steel girders, with 175 mm girder spacing for the first two models, which had curvature (L/R) of 0.2 and 0.3, respectively. The other three models had 200 mm girder spacing, with curvature of 0.1, 0.2 and 0.3, respectively. The applied loads were equivalent to the self-weight and superimposed dead load to achieve that of the full scale designed bridge plus one of the Iraqi bridge live load cases (Lane, Military loading: composed of tracked vehicles class 100 and wheeled vehicles class 100) sequentially. The experimental results revealed that the Iraqi Wheeled load case controlled the behaviour of most of the bridge models; all the girder deflections were below the permissible AASHTO LRFD 2012 limit. The longitudinal mid-span bottom flange girder strain was less than the girder yield strain and the maximum longitudinal mid-span concrete strain at the top surface was (469 micro-strains) which was lower than the ultimate concrete strain of (3000 micro-strains). The deflection and the longitudinal girder strains increased with the increasing curvature, whereas the girder spacing exerted only a very slight effect.

Keywords: Curved bridge, Composite section, Girder spacing, Rolled section.

1. Introduction

Horizontally curved in plan composite bridges (Concrete deck on steel I-girders) possess many beneficial properties including easy fabrication and construction, less land requirement during erection, and achievement of shallower sections.

Nomenclatures

ab	After cold bending
bb	Before cold bending
C1, C2, C3	degree of curvature, 0.1, 0.2, 0.3, radian
D_C	Diaphragm coupon
Es	Steel modules of elasticity, MPa
F_C	Flange coupon
G_1,G_2	Girder No. 1, 2 (Figs. 1 and 2)
G_3,G_4	Girder No. 3, 4 (Figs. 1 and 2)
KEL	Knife Edge Load, kN per lane
Las	Girder arch length, m
L/R	Span length to radius of curvature ratio, radian
S175, S200	Girder spacing, 175 and 200, mm
SIDL	Equivalent superimposed load, kN/m^2
Sw	Equivalent self-weight, kN/m^2
W_C	Web coupon
UDL	Uniform distributed load, kN/m per lane

Greek Symbols

ε_y	Girder yield strain, mm/mm
ε_u	Concrete compressive ultimate strain, mm/mm

Abbreviations

AASHTO	American Association of State Highway and Transportation Officials
FHWA	The Federal Highway Administration
ISS	Iraqi Standard Specification
LRFD	Load Resistance Factor Design

Besides, smaller loads are applied to the foundation when compared to the precast, prestressed beams or segmental prestressed concrete box girder deck. Also, the excellent serviceability performance of such types of bridges was proven to be an effective way of solving the intersection problems in cities [1]. Shanmugam et al. [2] investigated the failure mode under concentrated loads at mid-span by testing two sets of horizontally curved girders. The first set consists of rolled section, while the second set involves built-up sections. The results of the experimental part were compared with the Finite Element Analysis using ABAQUS software.

Thevendran et al. [3] investigated the ultimate load behaviour of horizontally curved steel-concrete composite beams. Five rolled steel beams of realistic dimensions with simply supported condition at the ends were tested till failure. The Federal Highway Administration (FHWA), in 1992, initiated an experimental and analytical approach for horizontally curved in plan steel bridges [4]. Full scale bridges of three-curved steel girders with simple supports and continuous boundary conditions were utilized in this study to investigate the real structural behaviour. Another approach adopted the field data collected, representing the response of the in-service three composite curved I-girder decks; the behaviours were investigated under live load traffic [5]. A comparison study between a two straight and an eight-curved plate girder, loaded at mid-span by a concentrated point load was performed by Shanmugam et al. [6]. A finite element analysis

using the ABAQUS software within the elastic-plastic range was performed and the results were compared with those obtained from the experimental approach.

The site measurements and results of the analysis for the horizontally in plan curved composite I-girder bridge decks were conducted by Hoffman [7]. The study involved one straight bridge and four curved bridges that were tested by strain transducers to determine the superstructure behaviour under the pattern of live loads. Investigation of the flexural behaviours under Iraqi Standard bridge live loads [8], by testing five bridge models was the principal aim of this study. The main variables were the girder spacing, and degree of curvature which is equal to (*L*/*R*), where *L* represents the central span length of the bridge model and *R* is the central radius of curvature.

2. Experimental Program

2.1. Manufacturing of the models

The scaled-down factor of (1/10) was adopted for scaling down the model dimensions from a full scale (Prototype) curved bridge with 30 m central span, 7.0 m carriageway width, 2.0 m girder spacing and an overall 1.64 m depth, including deck thickness. The prototype bridge was designed according to the AASHTO LRFD 2012 specifications [9] and subjected to the Iraqi Bridge live loads [8], as shown in Table 1. The bridge model dimensions are shown in Figs. 1 and 2 and the bridge model cross-section in Fig. 3 [10]. Using a rolled steel section (*IPN 120*) the bridge models were manufactured. First, the width of the top flange was reduced (from 64 mm to 50 mm) to simulate the prototype design requirements; second, the girder curvature was formed by employing cold bending processes in progressive and small increments of bend. The lengths of the steel girders in each bridge model are shown in Table 1. The diaphragms and transverse stiffeners were modelled using 2 mm thick steel plates. In the welding stage the fillet weld type E70XX was implemented to assemble the girders, diaphragms, stiffeners and shear connectors, utilizing a low temperature system to minimize the welding deformations. Finally, the wood formwork required was fixed to pour the deck concrete assembly onto the deck slab reinforcement as shown in Fig. 4.

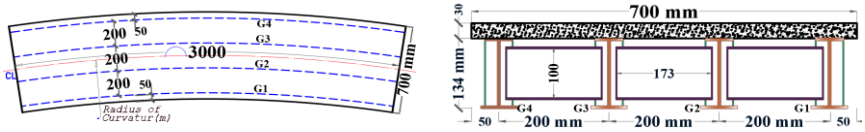

(a) Plan. **(b) Cross-section.**

Fig. 1. *S200* bridge model dimensions (Geometry and dimensions).

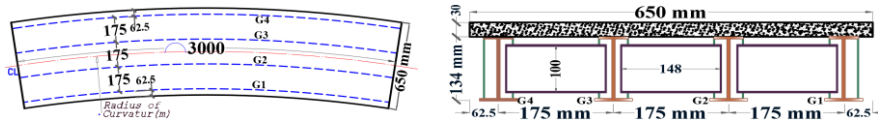

(a) Plan. **(b) Cross-section.**

Fig. 2. *S175* Bridge model dimensions (Geometry and dimensions).

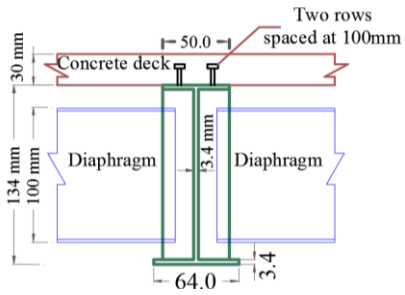

(a) Steel girder cross-section.

(b) Stiffener.

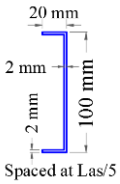

(c) Diaphragm cross - section.

Fig. 3. Typical bridge model cross - section.

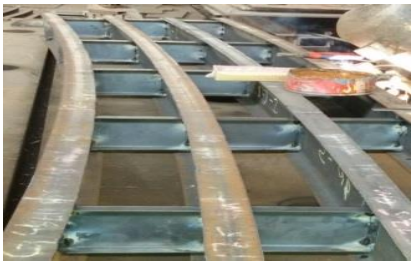

(a) Welding diaphragms.

(b) Welding the studs.

(c) Wood formwork.

(d) Casting the concrete.

Fig. 4. Assemblage of the bridge model components.

Table 1. Bridge models dimensions and properties.

Bridge models	Central Span (m)	Radius (m)	Curvature, *L/R* (radian)	Girder Spacing (mm)	Girders arch length, *Las* (m)			
					G_1	G_2	G_3	G_4
S200 C1	3.0	30	0.1	200	2.970	2.990	3.010	3.030
S200 C2	3.0	15	0.2	200	2.941	2.982	3.022	3.062
S200 C3	3.0	10	0.3	200	2.911	2.971	3.031	3.091
S175 C2	3.0	15	0.2	175	2.948	2.983	3.019	3.054
S175 C3	3.0	10	0.3	175	2.922	2.975	3.028	3.080

2.2. Material properties

The concrete strength of the deck was determined from three 150 mm cubes taken from each specimen. The concrete compressive strength at 28 days age was 35 MPa. To determine the tensile strength of the steel girders, a specimen was cut from the flange and web, both prior to and post cold bending for the three curvature values of 0.1, 0.2 and 0.3 radians, as shown in Table 2. The differences in the strength magnitude before and after the cold bending achieved 7.1 and 5.8% for yield stress and ultimate strength, respectively. Thevendran et al. [3] used a rolled I-section to model steel I-girder, for which the maximum deviation reached 18% for the yield stress and 9.4% for the ultimate strength. On the other hand, 3.4 mm thick steel plates were cut and welded to construct the built-up I-section girder, after which the coupons were prepared and tested to compare the differences in the tensile strength with that of the same coupons but without exposing them to the weld heating. The tensile yield stress was 418.9 MPa for the first coupon group, while it was 355 MPa for the welded ones. Therefore, the deviation was 18%; however, the difference when compared with that of the cold bent coupons was 7.1%. This implies that the temperature resulting from the welding process while building up a steel section influences the properties of that section, particularly in the case of small plate thickness in the fabrication of bridge models. The results of the tensile test of the reinforcement bars were 650 and 815.6 MPa for yield stress and ultimate strength, respectively.

Table 2. Mechanical properties of the bridge model coupons.

Properties	*L/R* = 0.10			*L/R* = 0.20			*L/R* = 0.30		
	F_C	W_C	D_C	F_C	W_C	D_C	F_C	W_C	D_C
Thickness (mm)	3.45	3.10	1.96	3.45	3.10	1.96	3.45	3.10	1.96
Yield stress, *bb* (MPa)	352.7	351.0	355.3	352.7	351.0	355.3	352.7	351.0	355.3
Yield stress, *ab* (MPa)	364.8	359.8		372.0	365.1		377.7	371.4	
% Of deviation, in yield stress	3.44	2.49		5.49	4.0	----	7.10	5.80	----
Ultimate strength, *bb* (MPa)	499.6	492.9	453.6	499.6	492.9	453.6	499.6	492.9	453.6
Ultimate strength, *ab* (MPa)	514.6	508.3	----	523.5	517.1	----	529.6	521.57	----
% Of deviation in ultimate stress	3.0	3.1	----	4.78	4.9	----	5.70	5.80	----
Elongation, *bb* %	14.6	13.9	17.2	14.6	13.9	17.2	14.6	13.91	17.16
Elongation, *ab* %	14.7	14.5	----	14.9	15.2	----	15.2	15.60	----

2.3. Instrumentation

Two sets of dial gauges each composed of four units, were used to determine the girder mid-span deflection, positioned at mid and end of the span under each girder. To confirm the complete connection and interaction between the concrete deck and the steel girders, as the models were designed, the Linear Variable Deferential Transformer (*LVDT*) was used at the end span of the model. To measure the mid-span longitudinal strain in the bottom flange girder, four

electrical resistances of 6 mm strain gauges were used. The mid-span longitudinal concrete strains above each girder were measured by using four electrical resistances of 60 mm strain gauges. The layout and location of the strain gauges in the bridge model are shown in Fig. 5. The readings of these strain gauges were displayed on the strain indicator, which was connected to a computer.

Rubber pads mounted on the *IPN220* steel section as a supporting beam were used to idealize the simply supported condition, as shown in Fig. 6. A manual 20-ton jack and a 30-ton capacity load cell were used and positioned between the top I-section (*IPN220*) and the bridge model to apply the equivalent Iraqi live loads, as shown in Table 3. In Fig. 6 the test rig elements are shown.

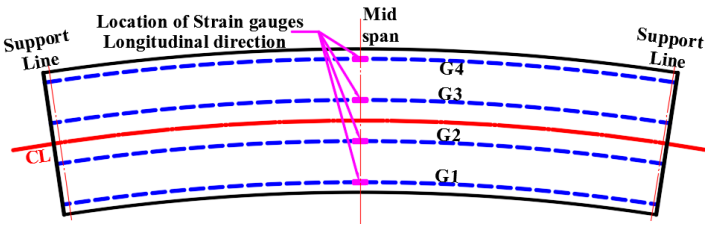

(a) Location of concrete strain gauges (Top view).

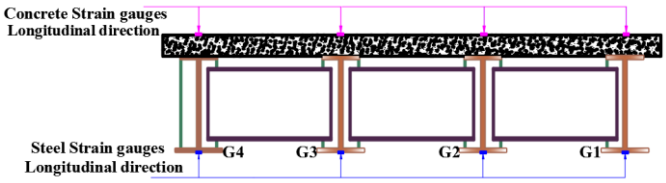

(b) Location of strain gauges (Mid-span cross-section).

Fig. 5. Location of the strain gauges for the bridge model.

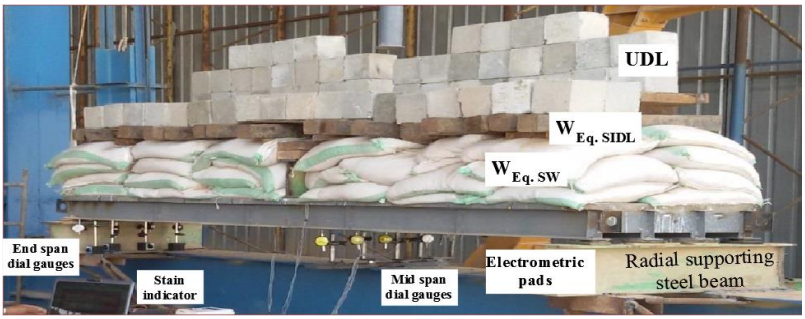

Fig. 6. Test rig elements.

2.4. Bridge live loads in accordance with the Iraqi Standards

Two bridge loading types, in accordance with the Iraqi Standards, were adopted in this study, for both lane and military loadings.

1. Lane loading includes the Uniform Distributed Load (*UDL* = 28.932 kN/m per lane) and Knife Edge Load (*KEL* = 120 kN per lane), as shown in Fig. 7(a), in accordance with the AASHTO LRFD 2012 limit; *UDL*= 9.33 kN/m per lane.

2. Military loading consisting of the tracked vehicles class 100 acts at mid-span, for a real total load of about 900 kN, as shown in Fig. 7(b), and wheeled vehicles class 100: This wheeled load acts longitudinally at the position to produce the maximum response of the bridge, when the real total load is 1150 kN, as shown in Fig. 7(c) in accordance with the AASHTO LRFD 2012 limit. The wheeled load is 320 kN and the design Tandem load is 222.4 kN.

To simulate the bridge self-weight, superimposed dead load and bridge live loads, two models were constructed using ANSYS Workbench 14.5 computer program [11]. One was for the full-scale curved bridge span to determine the stresses at the bottom flange of the steel girder. These stresses were then reflected on the second scaled-down model to evaluate the additional loads that must be applied to induce the same stresses as those in the full-scale bridge span. Accordingly, the live loads as indicated in Table 3 were adopted.

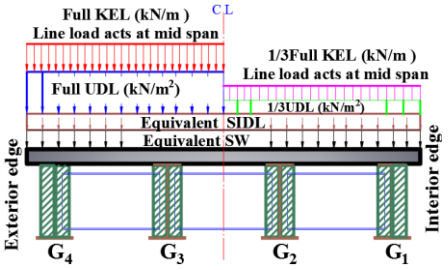

(a) Lane load application (Section at mid-span) with equivalent *Sw + SIDL*.

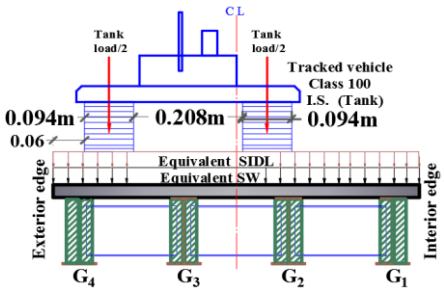

(b) Track class 100 load application (Section at mid-span) with equivalent *Sw + SIDL*.

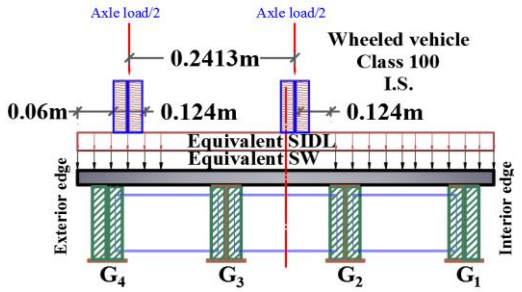

(c) Wheel load application (Section at mid-span) with equivalent *Sw + SIDL*.

Fig. 7. Modelled Iraqi live loads in addition to the self-weight and superimposed dead load.

2.5. Equivalent loads

As mentioned earlier, the equivalent loads were applied on the bridge model to induce the same longitudinal bottom steel flange stress as that of the full-scale bridge due to real self-weight S_w (1) and superimposed dead loads *SIDL* (2) and bridge live loads, 3-i, 3-ii and 3-iii, as listed in Table 3.

Table 3. Equivalent loads.

Bridge model	Equivalent dead loads		Equivalent Live loads			
	1	2	3-i		3-ii	3-iii
	Sw (kN/m^2)	*SIDL* (kN/m^2)	*UDL* (kN/m^2)	*KEL* (kN/m)	Tank (kN)	Wheel (kN)
S175C2	96	15.4	8.266	3.428	9.0	11.50
S175C3	96	15.4	8.266	3.428	9.0	11.50
S200C1	93	15.4	8.266	3.428	9.0	11.50
S200C2	93	15.4	8.266	3.428	9.0	11.50
S200C3	93	15.4	8.266	3.428	9.0	11.50

2.6. Test procedure

The experimental test procedure followed the fabricating of five simply supported scaled down bridge models by (1/10) of a prototype simply supported horizontally curved composite concrete -steel I-girder bridges, which were designed according to AASHTO LRFD 2012 standard specification and subjected to Iraqi Standard bridge live loads are summarized below:

a. First, the bridge model was mounted on the supporting elastomeric pads. The initial dial gauge and strain device readings were recorded and those for each load stage, as specified in Table 3.

b. Sandbags were employed to idealize the uniform equivalent self-weight, as shown in Fig. 6.

c. Steel shafts and steel blocks were used to idealize the equivalent superimposed dead load, as seen in Fig. 6.

d. Application of Live loads: The lane load was idealized by using a steel prism and concrete blocks applied as the full load on the exterior traffic lane and one-third on the interior traffic lane as the *UDL* and *KEL*, as shown in Fig. 10. The equivalent military Tracked Vehicle Class 100 (Tank) was idealized by using the steel double I-section (*IPN220*), as shown in Fig. 8. The equivalent load was applied using a manual jack, as evident from Fig. 11. The equivalent military Wheeled Vehicle Class 100 live load also was idealized using the steel double I-section (*IPN220*), as shown in Fig. 9. The point of load application coincided with the resultant action line. The equivalent load was applied by using a manual jack, as shown in Fig. 12.

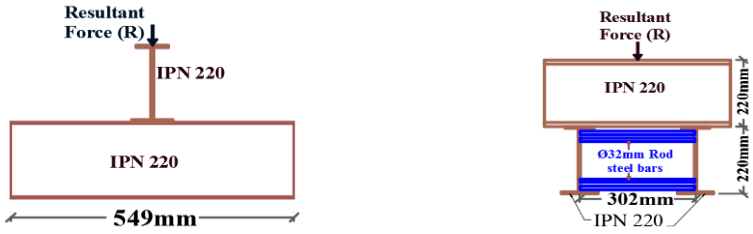

(a) Model longitudinal section. **(b) Model cross section.**

Fig. 8. Tracked vehicles class 100 (Tank) model.

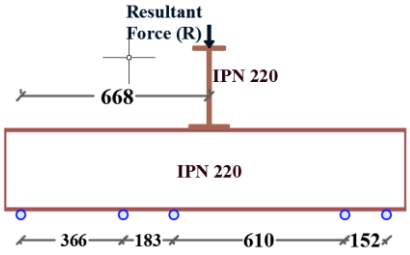

(a) Model longitudinal section.

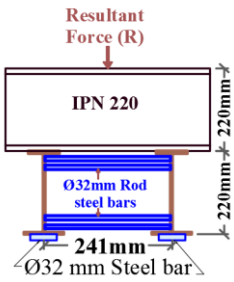

(b) Model cross section.

Fig. 9. Wheeled vehicles class 100 model.

Fig. 10. Equivalent *SW+SIDL* + Lane load.

Fig. 11. Equivalent *SW+SIDL+* Tank.

Fig. 12. Equivalent *SW+SIDL+* wheel loads.

3. Experimental Results and Discussion

3.1. Vertical deflection

All the test models (*S175 C2*, *S175 C3*, *S200 C1*, *S200 C2* and *S200 C3*) were loaded sequentially by the load stages as listed in Table 3. Figures 13 to 17 reveal the mid-span deflection of all girders of the bridge models under their own-weight with equivalent *Sw* (1), equivalent *SIDL* (2) and one of the equivalent live load cases. For the bridge model *S175C3*, the deflections of the outer girder G_4 relative to that of the inner one G_1 were 200, 202 and 214% for the loading stages of 3-i, 3-ii and 3-iii, respectively, which are higher than those reported for the bridge model *S175C2* (197, 189 and 200%). A similar observation was recorded for the bridge models with 200 mm girder spacing, where for bridge model *S200 C3*, the

relative deflection value of the outer to the inner girders was 201, 205 and 229% for the loading stages of 3-i, 3-ii and 3-iii, respectively, which are higher than the values for *C1* (140, 152 and 164%) and *C2* (181, 191 and 152%) curvature, implying that the deflection of the outer girder relative to that of the inner girder under live load increases when the curvature is increased and the wheel load is the control live load case. It is obvious that the inner girder G_1 had approximately the same deflection under all the instances of live loads for each bridge model, in contrast with that of the exterior girder.

3.2. Mid-span bottom flange girder strain

The maximum mid-span longitudinal strain generated in the bottom flange was (697 micro-strains) in the outer steel girder for the *S200 C3* bridge model under Wheel load, in addition to the equivalent *Sw* (1) and *SIDL* (2), which is below the girder yield strain and is shown as follows:

$$\varepsilon_y = \sigma_y / E_s = 374.61/200000 = 1873 \text{ micro} - \text{strains} > 697 \quad (1)$$

This suggests that all the processes of the loading stages of models own-weight with equivalent *Sw* (1), equivalent *SIDL* (2) and one of the live load cases fell within the elastic zone and no residual stresses were generated. Figures 18 to 22 show the mid-span longitudinal strain in the bottom flange of the steel girders. It is observed that, the relative longitudinal strains of the outer to the inner girders for bridge model *S175 C3* under the total equivalent dead and live load stages of 3-i, 3-ii and 3-iii were 173, 173 and 186%, respectively, while the values were 170, 167 and 188% for bridge model *S200 C3*. This implies that for the same curvature of *C3* [(*L*/*R*) = 0.3 radians], due to the increase in the girder spacing, there is a slight increase in the longitudinal girder bottom flange strain under the live load.

3.3. Mid-span top concrete strain

Figures 23 to 27 show the longitudinal strain at the top fibre of the concrete deck slab above the steel girders. The relative top fibre concrete longitudinal strains of the outer to the inner girders under the total equivalent dead and live loads for bridge model *S175 C3* were 337, 310 and 329% for the loading cases of 3-i, 3-ii and 3-iii, respectively, while they were 297, 292 and 269% for the bridge model *S175 C2*; a similar observation was reported for the bridge models of 200 mm girder spacing, implying that as the bridge curvature increases the top concrete deck slab strain also increases. The relative external to internal top concrete strain of *S200 C3* were 311, 293 and 339 micro-strains for the total equivalent dead and live load stages of 3-i, 3-ii and 3-iii, respectively, implying that girder spacing exerted very little influence when compared with that of the bridge curvature.

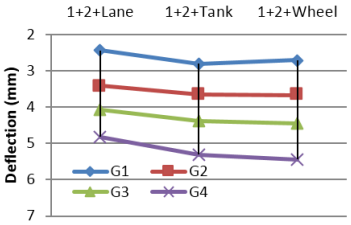

Fig. 13. Girders deflection -

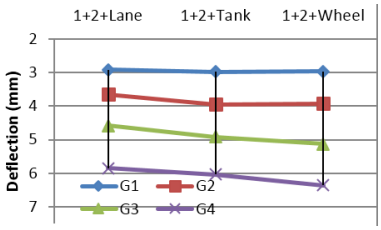

Fig. 14. Girders deflection - *S175C3*.

S175C2.

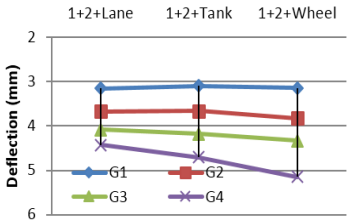

Fig. 15. Girders deflection - *S2005C1*.

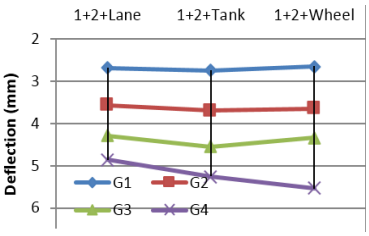

Fig. 16. Girders deflection - *S200C2*.

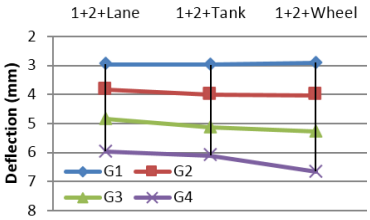

Fig. 17. Girders deflection - *S200C3*.

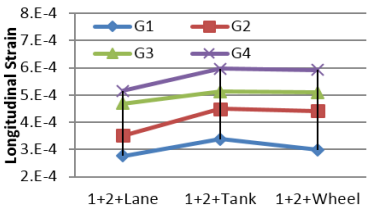

Fig. 18. Girders long. strain - *S175C2*.

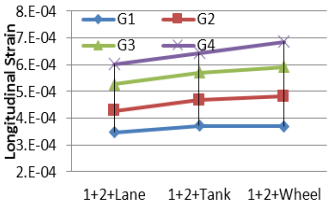

Fig. 19. Girders long. strain - *S175C3*.

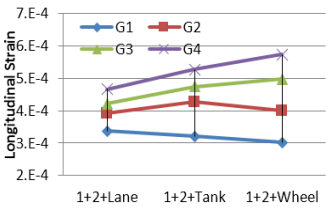

Fig. 20. Girders long. strain - *S200C1*.

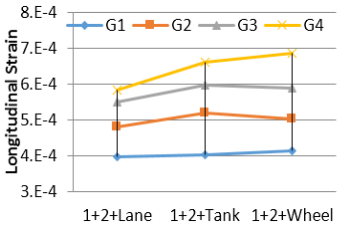

Fig. 21. Girders long. strain - *S200C2*.

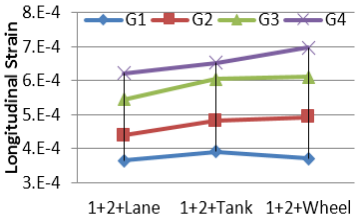

Fig. 22. Girders long. strain - *S200C3*.

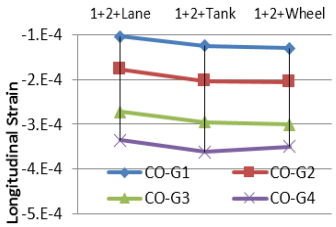

Fig. 23. Concrete long. strain - *S175C2*.

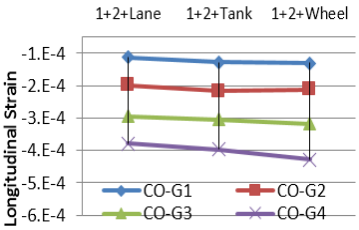

Fig. 24. Concrete long. strain -*175C3*.

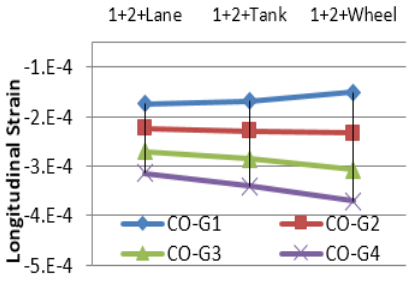

Fig. 25. Concrete long. strain - *S200C1.*

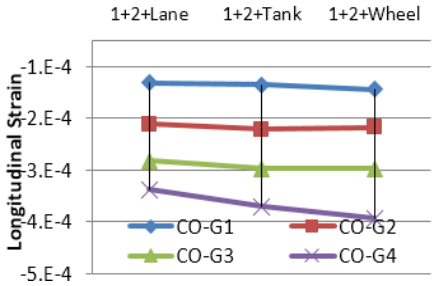

Fig. 26. Concrete long. strain - *S200C2.*

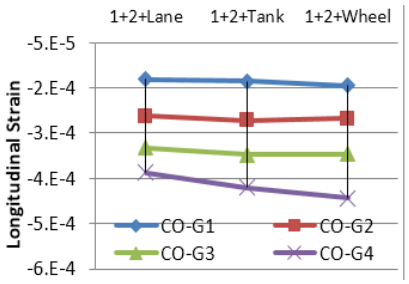

Fig. 27. Concrete long. strain - *S200C2.*

3.4. Comparison of the results of deflection

3.4.1. Deflection versus degree of curvature

Figures 28 to 30 show the deflection of the girders versus the degree of curvature of the bridge model. The main observation was that the deflection of the inner second girder G_2 remained appreciably unchanged and behaved as a fictitious point, whereas the deflection of girder G_1 showed a slight decrease with the increase in curvature; this was in contrast to the deflection of the outer girders G_3 and G_4, which showed significant increase.

3.4.2. Deflection versus girder spacing

Figures 31 to 33 show the deflection for the bridge models of (L/R) = 0.3 curvature for the three cases of live load with the equivalent dead loads versus girder spacing. It is evident that there were marginal increases in the deflection caused by the increase in the girder spacing. A slight difference was observed in girders G_2 and G_3 under Lane load, and girder G_3 and G_4 under the Tank and Wheel loads, respectively

3.4.3. Comparison with the AASHTO LRFD limit

All the values of the maximum net central deflection reported for the mid-span of the exterior girder for each bridge model resulting from the application of the live load cases were below the permissible AASHTO LRFD 2012 limit, as shown in Table 4.

Table 4. The net live load deflection of the exterior girder under only Iraqi standard bridge live loads for the bridge models and the AASHTO LRFD 2012 limitation

Bridge model	Span of exterior girder (mm)	Lane Load (mm)	Tank Load (mm)	Wheel Load (mm)	AASHTO LRFD 2012 limit, *L*/1000 (mm)
S175 C2	3054	1.99	2.48	2.61	3.05
S175 C3	3080	2.33	2.52	2.85	3.08
S200 C1	3031	1.70	1.98	2.42	3.03
S200 C2	3062	1.76	2.15	2.44	3.06
S200 C3	3091	2.35	2.50	3.04	3.09

3.5. Comparison of girders longitudinal strain results

3.5.1. Longitudinal bottom flange girder strain versus the degree of curvature

Figures 34 to 36 reveal the longitudinal girder strains versus the degree of curvature of the bridge models under both live and equivalent dead loads in the case of 200 mm girder spacing. The girder longitudinal strain was observed to increase with the increasing curvature of the bridge models, especially at the exterior girders than of the inner ones when the lane and tank loads were applied.

3.5.2. Longitudinal bottom flange girder strain versus girder spacing

Figures 37 to 39 show the longitudinal strain of the girder versus girder spacing under both live and equivalent dead loads in the case of L/R = 0.3. It is evident that for this instance of curvature a similar behaviour was exhibited under all types of live loads, implying that spacing between the girders has very little effect on the bottom girder strain.

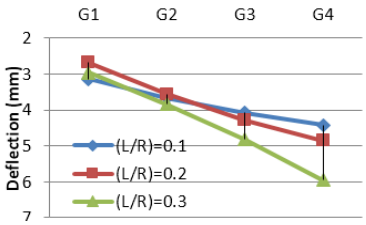

Fig. 28. Girders deflection - Lane load (*S200*mm).

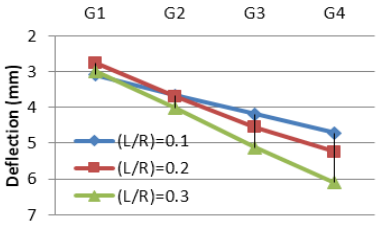

Fig. 29. Girders deflection - Tank load (*S200*mm).

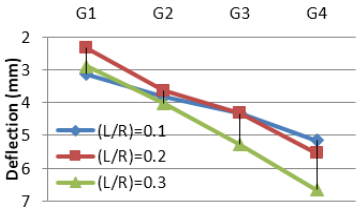

Fig. 30. Girders deflection - Wheel load (*S200*mm).

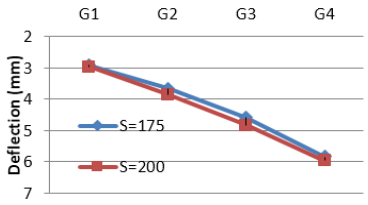

Fig. 31. Girders deflection - Lane load (L/R = 0.3).

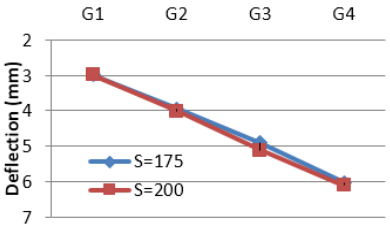

Fig. 32. Girders deflection- Tank load (*L/R* = 0.3).

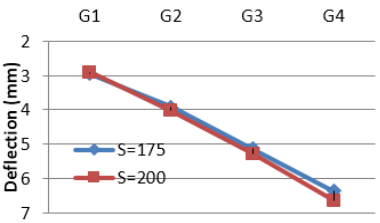

Fig. 33. Girders deflection - Wheel load (*L/R* = 0.3).

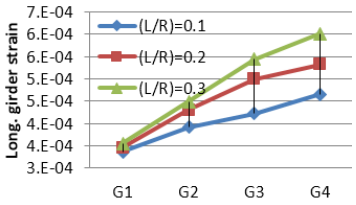

Fig. 34. Girders long. strain- Lane load *S200*mm.

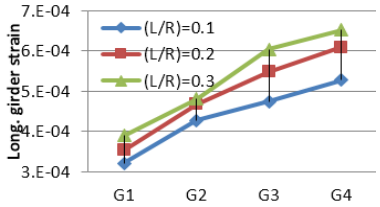

Fig. 35. Girders long. strain - Tank load *S200*mm.

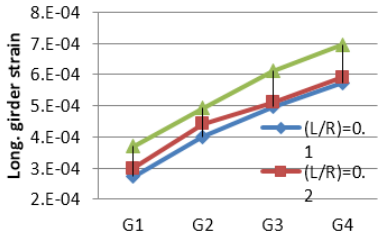

Fig. 36. Girders long. strain - Wheel load *S200*mm.

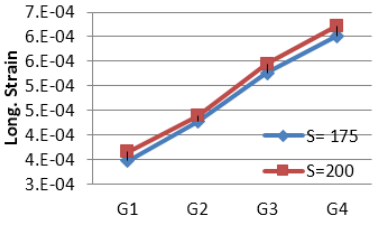

Fig. 37. Girders long. strain - Lane load (*L/R* = 0.3).

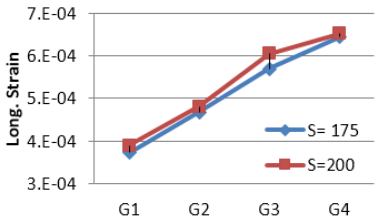

Fig. 38. Girders long. strain - Tank load (*L/R* = 0.3).

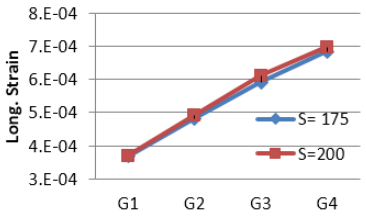

Fig. 39. Girders long. strain - Wheel load (*L/R* = 0.3).

4. Conclusions

According to the experimental programme which has been made to study the flexural behaviour of horizontally in plan curved composite bridges (concrete deck on steel I-girder) under Iraqi live loads the following conclusions can be driven:

- **Mid-span girder deflections.** The girders deflection results due to applying Iraqi live load within the limit of AASHTO LRFD 2012 for all tested bridge model. With the application of the live load and by increasing the degree of curvature of the bridge model, the mid-span cross-section was observed to show a tendency to rotate towards the external side of the curvature, and this phenomenon increased as the bridge curvature was increased. The deflection of interior girder, however, remained largely unchanged and acted as a fictitious point with the application of the live load and increasing the degree of curvature of the bridge model. The deflection of the inner girder showed a slight decrease; however, by contrast, the deflection of the outer girders was seen to significantly increase. No girder tilting (uplift) was measured for all the cases of Iraqi live load application. The results of the girder deflections due to the application of Iraqi live load within the AASHTO LRFD 2012 limit are shown. Therefore, it is possible to apply the AASHTO LRFD design and limitation philosophy to the live loads of the Iraqi Standard Bridge
- **Mid-span longitudinal girder strain.** All the girder strains generated fell below the girder yield strain, implying that the design of the curved I-girder bridge according AASHTO LRFD limit for Iraqi live loads were within the elastic zone. The experimental results show that the longitudinal girder strains increased as the bridge curvature increased, because of the increase in the torque generated in the bridge section; the spacing between girders, however, was found to exert very minimal effect on longitudinal girder strain.
- **Mid-span longitudinal concrete strain.** The maximum compressive concrete strain generated under all the Iraqi live loads tested was 469 micro-strains for the bridge models tested, which is below the maximum compressive concrete strain (3000 micro-strains). The experimental results reveal that the top surface compressive concrete strain increases with the increase in the bridge curvature under live loads, especially just above the exterior girder; girder spacing, however, was observed to exert very little influence on the longitudinal compressive concrete strain at the top surface of the deck slab above the steel girder.

References

1. Nick, H.; and Jessica, W.D. (2012). S*teel girders.* MnDOT Bridge Office LRFD Workshop.
2. Shanmugam, N.E.; Thevendran, V.; Richard Liew, J.Y.; and Tan, L.O. (1995). Experimental study on steel beams curved in plan. *Journal of Structural Engineer*, 121(2), 249-59.
3. Thevendran, V.; Shanmugam, N.E.; Chen, S.; and Richard Liew, J.Y. (2000). Experimental study on steel-concrete composite beams curved in plan. *Engineering Structures*, 22(8), 877-889.
4. Zureick, A.; Linzell, D.; Leon, R.T.; and Burrell, J. (2000). Curved steel I-girder bridges: experimental and analytical studies. *Engineering Structures*, 22(2), 180-190.

5. Mclwain, B.A.; and Laman, J.A. (2000). Experimental verification of horizontally curved girder bridge behavior. *Journal of Bridge Engineering*, 5(4), 284-292.
6. Shanmugam, N.E.; Mahendrakumar, M.; and Thevendran, V. (2003). Ultimate load behaviour of horizontally curved plate girders. *Journal of Constructional Steel Research*, 59(4), 509-529.
7. Hoffman, J.J. (2013). *Analytical and field investigation of horizontally curved girder bridges*. M.Sc. Thesis. Civil, Construction, and Environmental Engineering, Iowa State University.
8. Iraq Standard Specification for Road Bridges (Loading), (1978).
9. American Association of State Highway and Transportation Officials, AASHTO (2012). Standard Specifications for Highway Bridges (6^{th} ed.). Washington D.C, *AASHTO LRFD Bridge Design Specification*.
10. Harry, G.; and Gajanan, M. (1999). *Structural modelling and experimental techniques*. (2^{nd} ed.). Washington D.C.: CRC press.
11. Izzet, A.F.; and Mohammed, A.R. (2016). Distribution factor of curved I-girder bridges under Iraqi Standard Bridge Live Loads. *Journal of Civil Engineering Research*, 6(3), 61-71.